PMAS
Proceedings of the Mongolian Academy of Sciences
Vol. 59 No 04 (232) 2019
DOI: https://doi.org/10.5564/pmas.v59i4.1291

ARTICLE

The Shape Analysis at One End of the Flux Tube with Dynamical Quarks

Battogtokh Purev*, Sodbileg Chagdaa and Enkhtuya Galsandorj

Institute of Physics and Technology, Mongolian Academy of Sciences
Ulaanbaatar, Mongolia

ARTICLE INFO: Received: 25 Oct, 2019; Accepted: 10 Mar, 2020

Abstract: *In the deconfinement phase transition, we have analyzed the shape of the one end of the flux tube computed by HISQ configurations in full QCD with (2+1) flavors. The ratio of the longitudinal and transverse profile of the parallel chrome-electric field strength revealed that the transverse profile becomes wider than the longitudinal profile when the temperature increases. Also, we found that the comparison, as a function of the distance between two quarks, likely shows melting distances of the flux tube. The melting distances are different for each temperature. They are R = 1.5 fm at T/T_c = 0.97 and R = 1.2 fm at above the critical temperatures T/T_c = 1.00, 1.03, 1.06 and 1.09.*

Keywords: *Full QCD; strong interaction; confinement; flux tube; critical temperature;*

INTRODUCTION

Shape analysis of the flux tube has always played an important role in the study of the confinement phenomenon. In this work, we have investigated shape changes at one end of the flux tube through the deconfinement phase transition. It can give us some useful information about the mechanism of confinement.

In the lattice numerical simulation, the flux tube is extracted from the correlation of a plaquette with the Polyakov loops

$$f_{\mu\nu}(R,x) = \frac{\beta}{a^4}\left[\frac{\langle L(0)L^{\dagger}(R)P_{\mu\nu}(x)\rangle}{\langle L(0)L^{\dagger}(R)\rangle} - \langle P_{\mu\nu}(x_{ref})\rangle\right],$$

by varying the orientation (μ,ν) of the plaquette $P_{\mu\nu}(x) = \frac{1}{N_c}TrU(x)$ and the distance x with respect to the Polyakov loop $L(x) = \frac{1}{N_c}Tr\prod_{\tau=1}^{N_\tau}U(x,\tau)$. Here a and β are lattice spacing and coupling constant, respectively.

***corresponding author: pbattogtokh@gmail.com** **https://orcid.org/0000-0002-5170-1267**

PMAS
Proceedings of the Mongolian Academy of Sciences
Vol. 59 No 04 (232) 2019
DOI: https://doi.org/10.5564/pmas.v59i4.1291

Two-dimensional picture of the flux tube is illustrated in Figure 1, where one can easily read off the longitudinal distance $x_{\parallel}$ and the transverse distances $x_{\perp}$ of the plaquette from the quarks. From the orientation (μ, ν) which has six values (1,4), (3,4), (2,4), (2,3), (1,3) and (1,2), field strength tensor $f_{\mu\nu}$ express chromo-electric field strength components $f_{14} = \frac{1}{2}E_{\parallel}^2, f_{34} = \frac{1}{2}E_{\perp}^2, f_{24} = \frac{1}{2}E_{\perp}^2$ and chromo-magnetic field strength components $f_{14} = -\frac{1}{2}B_{\parallel}^2, f_{13} = -\frac{1}{2}B_{\perp}^2, f_{12} = -\frac{1}{2}B_{\perp}^2$. Several studies [1-4] revealed that the parallel chromo-electric field strength is always larger than all other field strengths, as well as the main component of the structure of the flux tube. Therefore, we have chosen profiles of only the parallel chromo-electric field strength at the one end of the flux tube in our analysis to explore the shape changes of the flux tube.

In one of our first studies [5], we investigated the shape of the one end of the flux tube in SU (2) pure gauge theory. In this work, we hanalyzed the one end of the flux tube with dynamical quarks configurations in full QCD with (2+1) flavors, using HISQ/tree action. Because of the discretization of the quark action in the lattice, the field strength distributions are affected by ultra-violet fluctuations. We used the gradient flow method [6,7] to reduce the statistical errors which is degenerated by this fluctuation. The net statistical errors of the field strengths were estimated by the Jackknife algorithm [7], in as much as the configurations were correlated.

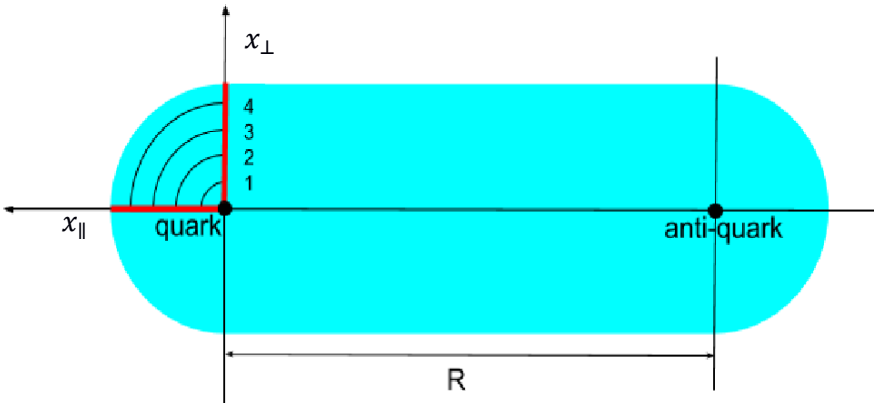

Figure 1. The two dimensional projection of the flux tube

ANALYSIS OF THE SHAPE

In this work, we have compared points from the longitudinal and transverse profile of $1/2E_{\parallel}^2$ at one end of the flux tube. The longitudinal $x_{\parallel}$ and transverse $x_{\perp}$ distributions at the source are drawn by vertical and horizontal red lines and the equal distance points along the lines are numbered by **1, 2, 3** and **4** in the Figure 1. Coordinates of the pairs of points are $\mathbf{1} \rightarrow \{(8a, 1a), (7a, 0)\}$, $\mathbf{2} \rightarrow \{(8a, 2a), (6a, 0)\}$, $\mathbf{3} \rightarrow \{(8a, 2a), (5a, 0)\}$ and $\mathbf{4} \rightarrow \{(8a, 4a), (4a, 0)\}$.

Now let's denote ratios of the transverse points of $1/2E_{\parallel}^2(8a, x_{\perp})$ and longitudinal points of $1/2E_{\parallel}^2(x_{\parallel}, 0)$ at each point as follows:

$$\{1\} \rightarrow E_{\parallel}^2(8a, 1a)/E_{\parallel}^2(7a, 0)$$
$$\{2\} \rightarrow E_{\parallel}^2(8a, 2a)/E_{\parallel}^2(6a, 0)$$
$$\{3\} \rightarrow E_{\parallel}^2(8a, 3a)/E_{\parallel}^2(5a, 0)$$
$$\{4\} \rightarrow E_{\parallel}^2(8a, 4a)/E_{\parallel}^2(4a, 0)$$

This ratio can present how the shape of the one end of the flux tube changes through the rising temperature and distance.

PMAS
Proceedings of the Mongolian Academy of Sciences
Vol. 59 No 04 (232) 2019
DOI: https://doi.org/10.5564/pmas.v59i4.1291

RESULTS AND DISCUSSION

In this work, we used our flux tube data which were simulated on the lattice of volume 32^3x8 for the five different temperatures T/T_c = 0.97, 1.00, 1.03, 1.06 and 1.09 and seven distances R/a = 4, 6, 8,10, 12, 14 and 16 in QCD with dynamical quark configurations. The gradient flow method suppressed the static noise of the configuration at the flow time t=0.25.

We have depicted four ratios as a function of the distance at five different temperatures in Figure 2. The first two plots showed that the ratio {1} and {2} decreased to a certain value of the distance at all the temperatures.

In other words, the longitudinal profile becomes larger or the longitudinal profile becomes thinner. These plots show that the ratio decreased linearly until the distance reaches R = 1.5 fm or R = 1.3 fm after that it is raised slowly below the critical temperature $T=0.97T_c$. Besides the above critical temperature, the ratio declined to distance R=1.2 fm, and thereafter it did not depend on distance. These distances are likely melting points of the flux tube for any temperature. Next two plots noted as {3} and {4} did not show proper relation as seen in the plots {1} and {2}.

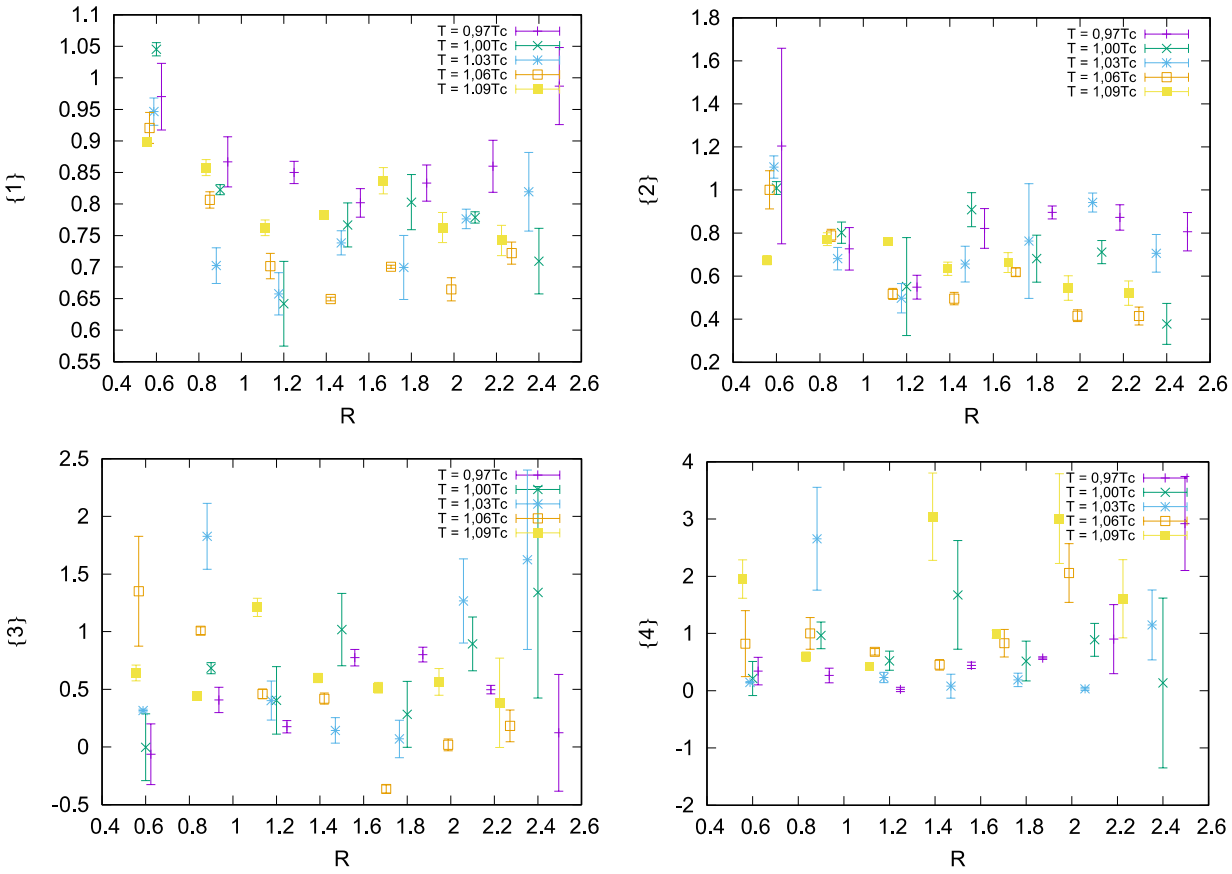

Figure 2. The ratio $E_{\parallel}^2(8a, x_{\perp})/E_{\parallel}^2(x_{\parallel}, 0)$ *as a function of distance*

PMAS
Proceedings of the Mongolian Academy of Sciences
Vol. 59 No 04 (232) 2019
DOI: https://doi.org/10.5564/pmas.v59i4.1291

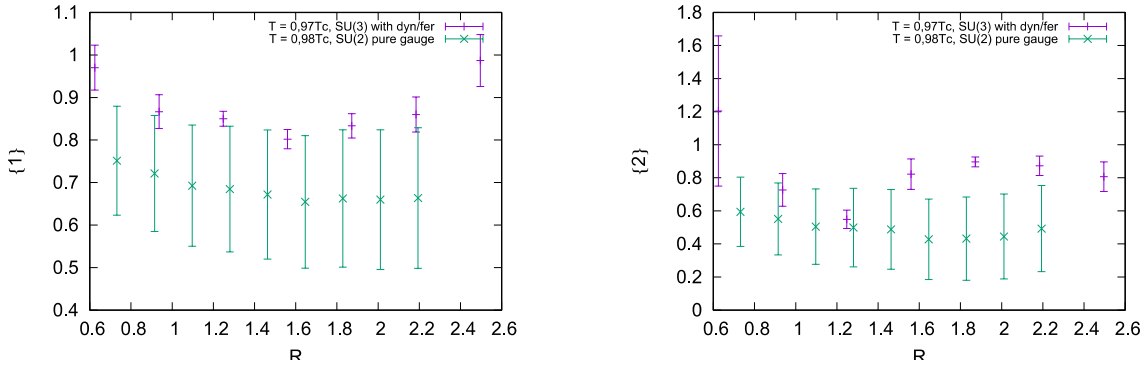

Figure 3. Comparison of SU(2) gauge results and SU(3) full QCD with (2+1) flavors results

We have presented results from our investigation. Here results of our previous work [5] of SU(2) pure gauge flux tube at T=0.97T_c is also inserted in Figure 3 for comparison purpose. The right and left plots respectively show comparisons of {1} and {2}. From the plot we can see that the ratios of the old study have been suppressed with the new ratios until the same distance after they have become constant. The difference of the comparison is shown in the growth of the ratios which included the dynamical quarks. The growth can likely express that the gluons are affected by the strong interaction of the quark after string breaking below the critical temperature.

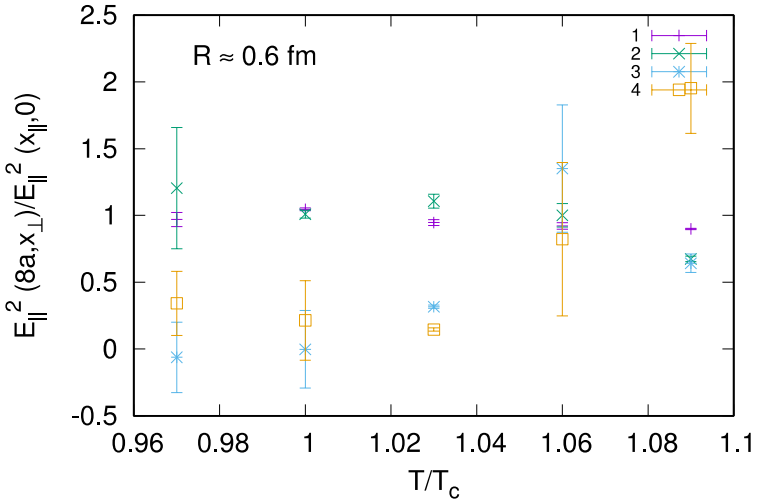

Figure 4. The ratio $E_{\|}^2(8a,x_\perp)/E_{\|}^2(x_{\|},0)$ as a function of temperature

The dependence of ratio on temperature is presented in Figure 4, which stands at R=0.6 fm. The first two ratios {1} and {2} did not depend on temperature while they were relatively equal. Whereas, ratios {3} and {4} strongly depend on temperature. The figure shows that at low temperatures, the longitudinal profile is wider than the transverse profile, but at a higher temperature, the longitudinal profile is thinner than the transverse profile.

CONCLUSIONS

We have studied the variation of the shape at one end of the flux tube as a function of temperature and distance. As a result of the ratios, we can conclude that the longitudinal

Vol. 59 No 04 (232) 2019
DOI: https://doi.org/10.5564/pmas.v59i4.1291

distribution of the flux tube is wider than the transverse distribution through the rising distances. Moreover, longitudinal distribution becomes finer than the transverse distribution when the temperature increases at a small distance.

Also, the dependence of the ratio on distance showed us some interesting points that may identify phase transition.

These points are R=1.5 fm and R=1.2 fm respectively below the T_c and above the T_c. We considered that when the flux tube breaks, the shape of one end of the flux tubedoes not change, owing to the disappearance of the strong interaction. However, below the critical temperature, the ratio grows from which it can be inferred that the strong interaction may still affect gluons and quarks after the flux tube breaks.

REFERENCES

1. Sommer R., Scaling of SU(2) flux distribution and potential, Nucl. Phys. B306 (1988), pp. 181-198.
2. Chagdaa S., Galsandorj E, Laermann E. and Purev B., Width and string tension of the flux tube in SU(2) lattice gauge theory at high temperature, J. Phys. G 45 (2017) 025002.
3. Cea P., Cosmai L., Cuteri F. and Papa A., Flux tubes at finite temperature, JHEP 06 (2016) 033, [arXiv:hep-lat/1511.01783].
4. Cosmai L., Cea P., Cuteri F., and Papa A., Flux tubes in QCD with (2+1) HISQ fermions, PoS (LATTICE2016) (2016) 344, [arXiv:heplat/1701.03371].
5. Battogtokh P., Sodbileg Ch., Edwin L., and Daariimaa B., The detailed analysis on the shape of the flux tube, Mongolian Journal of Physics issue 2 (2016), p. 464.
6. Lьscher M., Properties and uses of the Wilson flow in lattice QCD, JHEP 08 (2010) 071, [arXiv:hep-lat/1006.4518].
7. Mazur L., Applications of the Gradient flow method in lattice QCD, Master's thesis, Bielefeld University (2017).
8. Huescher.M Trivializing maps, the Wilson flow and the HMC algorithm, Comm. Math. Phys. 293 (2010) 899-919, [arXiv:hep-lat/0907.5491].